Poly(styrene-*b*-methyl methacrylate) block copolymers as compatibilizing agents in blends of poly(styrene-*co*-acrylonitrile) and poly(2,6-dimethyl-1,4-phenylene ether): 1. Location of block copolymers in ternary blends — compatibilization *versus* micelle formation

Clemens Auschra and Reimund Stadler*
Institut für Organische Chemie, Johannes-Gutenberg-Universität, J. Becherweg 18–20, W-6500 Mainz, Germany

and Ingrid G. Voigt-Martin
Institut für Physikalische Chemie, Johannes-Gutenberg-Universität, Welderweg, W-6500 Mainz, Germany
(Received 12 September 1991; revised 3 August 1992)

The compatibilizing effect of the symmetric narrowly distributed block copolymer poly(styrene-*b*-methyl methacrylate) (P(S-*b*-MMA)) in blends of high-molecular-weight poly(styrene-*co*-acrylonitrile) containing 20 wt% (PSAN20) or 43 wt% acrylonitrile (PSAN43) with poly(2,6-dimethyl-1,4-phenylene ether) (PPE) was investigated by dynamic mechanical spectroscopy and transmission electron microscopy. In blends with the PSAN43, P(S-*b*-MMA) forms spherical micelles in the PPE phase with no dispersing efficiency. In contrast to this, for blends with PSAN20, the block copolymer is located at the phase boundary, causing an extremely fine dispersion of the components. Depending on the location of P(S-*b*-MMA), the PPE glass transition is altered by the PS blocks to different degrees. Even for block copolymer concentrations as high as 20 wt%, in ternary blends with PSAN20 and PPE no micelles could be detected. The results suggest that A/B blends compatibilized with a C-D block copolymer, in which the copolymer components show an exothermic heat of mixing with the bulk phases A/B, are superior to systems A/A-B/B with respect to emulsifying efficiency. Owing to the high tendency of the block copolymer to locate at the phase boundary, micelles do not compete at concentrations of practical interest.

(Keywords: block copolymers; compatibilizers; blends; poly(styrene-*b*-methyl methacrylate); poly(styrene-*co*-acrylonitrile); poly(phenylene ether); morphology; ternary blends; micelle formation)

INTRODUCTION

Multiphase polymer blends are of great importance in the development of new synthetic materials. However, the realization of new useful alloys is severely limited by the strong incompatibility of many polymer pairs of interest. For many systems, high interfacial tension and weak phase adhesion lead to ill-defined morphologies with coarsely phase-separated structures and inferior ultimate mechanical properties.

One of the basic problems is to improve the adhesion across the phase boundary with better control of morphology. This can be achieved by appropriate interfacial agents like block or graft copolymers that locate at the interface and anchor the phases[1]. The molecular characteristics of the compatibilizer, i.e. block architecture, molecular weight and chemical composition, are the key parameters to be optimized in order to get high efficiency[2]. Much work has been done on systems in which the blocks of the compatibilizer are chemically identical to the bulk phases and has proven to be successful[3,4]. A major drawback of this approach is the fact that above a certain threshold concentration, *CMC* (critical micelle concentration), the block copolymers prefer to segregate into micelles in one (or both) blend components, rather than to stick to the interface[5,6]. Thus, above the *CMC*, which can be relatively low, an increase of copolymer concentration will not lead to further improvement of the adhesion across the phase boundary.

Detailed self-consistent mean-field calculations of Hong and Noolandi[7] for a quaternary system A/A-B/B with non-selective solvent, as well as the approaches of Leibler[8] and Shull and Kramer[9] for a ternary A/A-B/B system, predict strong reduction of interfacial tension with increasing block copolymer molecular weight and/or concentration until the *CMC* is reached. The *CMC* itself

* To whom correspondence should be addressed

0032-3861/93/102081-13

follows the opposite trend, in that the *CMC* value decreases with increasing copolymer molecular weight.

In view of these equilibrium thermodynamic theories, the best compatibilizer with respect to the reduction of interfacial tension in a system of high-molecular-weight polymer A and B is a symmetric diblock copolymer A-B, which has to be long enough to reduce significantly the interfacial tension, but still short enough to avoid micelle formation. However, owing to the non-equilibrium nature achieved under normal processing conditions, it is possible that kinetic effects will severely limit the effectiveness of compatibilizers, e.g. diffusion problems of large block copolymers. In extension of this concept, systems A/A-C/B[10,11] and A/C-D/B[12], in which one or both blocks of the compatibilizer are chemically different from, but miscible with, the blend components, are receiving increasing attention.

Random copolymers of styrene and acrylonitrile (PSAN) and poly(2,6-dimethyl-1,4-phenylene ether) (PPE) are familiar components frequently used in engineering polymer blends. Blends of PSAN and PPE could offer an interesting combination of properties if the mechanical incompatibility could be overcome. In contrast to the well established miscibility of polystyrene (PS) and PPE[13–15], the incorporation of acrylonitrile (AN) units into PS rapidly decreases miscibility owing to the unfavourable interaction of AN segments and PPE. Miscibility as indicated by the observation of a single glass transition was demonstrated for 50:50 blends up to 10–12 wt% AN in the PSAN copolymer[16]. Block copolymers of styrene and methyl methacrylate (P(S-*b*-MMA)) can be expected to act as compatibilizers for incompatible blends of PSAN20 (PSAN containing 20 wt% AN) and PPE, because each block is selectively miscible with one of the component phases.

Depending on the AN content in the copolymer, PSAN and PMMA show a miscibility window between approximately 9 and 30 wt% AN[17–19]. Ternary blends containing PSAN of this composition range, PPE and P(S-*b*-MMA) represent an amorphous A/C-D/B model system with an exothermic heat of mixing of the blocks with the bulk phases. There are several advantages to a systematic investigation of the blend behaviour in this model system: (1) Well defined P(S-*b*-MMA) block copolymers are accessible by sequential anionic polymerization. (2) The incompatibility of the bulk components can be continuously varied by changing the AN content of PSAN, i.e. from weak to strong segregation. (3) The interaction of the PMMA block with PSAN is also controlled by the AN level in PSAN. (4) The glass transitions of PSAN, PS and PMMA are well separated from the PPE glass transition, which depends sensitively on the mixing behaviour of PS blocks and PPE.

By the use of defined blend components, i.e. anionically prepared block copolymers and fractionated high-molecular-weight samples of PSAN and PPE, we intend to evaluate the mechanical and morphological behaviour of the ternary blends. Other attempts along the same lines have been reported using ternary blends of PSAN15, PPE and P(S-*b*-MMA)[20]. The compatibilizing effect was concluded from the lowering of the PPE glass transition measured by d.s.c. and morphological characterization by SEM. The possibility of micelle formation in the PPE phase, which would also lower the T_g of PPE, was not examined. The use of P(S-*b*-MMA) to compatibilize blends of PSAN and PPE is also described in the patent literature[21].

In this paper we investigate the location of a symmetric high-molecular-weight P(S-*b*-MMA) copolymer in ternary blends with high-molecular-weight PSAN and PPE by means of dynamic mechanical spectroscopy and TEM. Special emphasis was directed to the question whether or not P(S-*b*-MMA) has a tendency for micelle formation rather than moving to the interface. First we make a rough estimation of the enthalpic interactions between the different polymer chains, which will determine the mixing behaviour of the block copolymer in the ternary blends. A binary blend based on PSAN20/PPE will be used to demonstrate how sample preparation and thermal history influence the dynamic mechanical and morphological behaviour. The effects of P(S-*b*-MMA) in ternary blends with PSAN and PPE are examined for comparison in blends PSAN20/PPE (60:40) and PSAN43/PPE (60:40) with relatively high amounts of P(S-*b*-MMA) (10 and 20 wt%).

EXPERIMENTAL

Materials

P(S-b-MMA). These block copolymers were prepared by sequential anionic polymerization in tetrahydrofuran (THF) at low temperature. The basic equipment consists of a 1.6 litre stirred, argon pressurized glass reactor with a thermostated cooling jacket. Technical-grade THF was predried by distillation from CaH_2, further purified by reflux over potassium and directly distilled into a flask connected with the reactor. Styrene and MMA were reagent grade, purified by standard procedures[22,23] with $MgBu_2$ and $AlEt_3$, respectively, and kept in Teflon-stoppered ampoules for short-term storage at liquid-nitrogen temperature.

Polymerization of styrene was initiated at −85°C with s-BuLi. After 20 min the PS block was capped with 1,1-diphenylethylene. For analytical purposes a small amount of the first PS block was taken from the reactor before the desired amount of MMA was slowly added. Depending on the intended molecular weights, total monomer concentration was in the range 5–8 wt/v. After 20 min, the polymerization was terminated by precipitating the mixture into 10-fold excess of water. The detailed description of the analytical procedures and an examination of the thermal stability of the P(S-*b*-MMA) block copolymers will be given elsewhere[24].

PPE. PPE was synthesized according to the method of Percec *et al.*[25] by phase-transfer catalysed polymerization of 4-bromo-2,6-dimethylphenol, which itself was prepared from 2,6-dimethylphenol by bromination[26]. In comparison with technical-grade PPE, this method leads to better defined high-molecular-weight PPE, which does not have the structural irregularities of technical-grade PPE, like branching[27], incorporated catalyst residues[28], etc. Owing to the molecular redistribution reaction of PPE[29], a successful fractionation is only possible if the free phenolic chain ends are reacted with a suitable capping agent[30]. For the quantitative alkylation of the free phenolic chain ends we developed a simple procedure in analogy to the phase-transfer catalysed alkylation of sterically hindered phenols with dialkylsulfates[31].

In a typical procedure an emulsion is prepared from a concentrated solution (>30% w/v) of PPE (50 g,

$M_n = 17\,000$, 3 mmol phenolic end-groups) and a 100-fold excess of 50% NaOH (12 g NaOH, 0.3 mol) and 2.04 g of NBu_4HSO_4 (6 mmol). Then 5 ml Me_2SO_4 (52 mmol) are slowly dropped into the mixture under vigorous stirring. Stirring is continued for 3 h. Before work-up, 40 ml of conc. NH_3 solution are added and stirred for 1 h to ensure the aminolysis of excess dialkylsulfate. For simpler handling, the mixture is diluted with 300 ml toluene and 300 ml H_2O and the water phase is removed. The toluene phase is washed twice with 300 ml H_2O (separation of the phases by centrifugation) and precipitated in excess methanol.

Fractionation of the end-capped PPE was performed by fractionated precipitation from dilute (<1% w/v) toluene solution with petroleum ether. The main goal of this procedure was to remove the low-molecular-weight portions. The fractionated sample PPE-I ($M_n = 43\,000$, $M_w/M_n = 1.5$) gave no evidence for broadening of the molecular-weight distribution under conditions where an uncapped PPE would redistribute (14 days in warm toluene solution with air contact). This is a strong indication for a quantitative end-capping.

PSAN20 and PSAN43. These were technical-grade copolymers from BASF and fractionated in the same way as PPE in order to remove low-molecular-weight portions. We found no indications of chemical inhomogeneities in the samples.

Characterization of polymers

Characterization was accomplished with g.p.c. ($CHCl_3$ or THF, r.i./u.v. detection, PS calibration), membrane osmometry ($CHCl_3$, THF), ^1H n.m.r. and elemental analysis. Characterization of the starting materials is given in *Table 1*.

Blend preparation

All blends were prepared by coprecipitation of the components from a warm THF solution (1.5% w/v) into a 10-fold excess of MeOH. The dried fine powders (vacuum, 80°C, >2 days) were melt pressed in a vacuum hydraulic press at 240°C for 45 min in special moulds to make the specimen for dynamic mechanical testing. It has been demonstrated that under these conditions the blends approach equilibrium without excessive degradation of P(S-*b*-MMA) (see below). Care was taken to ensure identical thermal history of all samples. Sample designation and details of the preparation conditions of the blends are summarized in *Table 2*.

Dynamic mechanical testing

The measurements were performed on a Rheometrics Solids Analyzer RSA2 in the temperature-step mode at a constant frequency of 1 rad s^{-1} and a delay time of 1 min before each measurement. Strains were kept small enough to ensure linear viscoelastic behaviour. To cover the mechanical behaviour over both glass transitions, the blends were tested with two different test geometries: dual cantilever (45 mm × 6 mm × 2.3 mm) for the modulus region with $E' > 10^8$ Pa and shear sandwich (2 × (2 mm × 5.5 mm × 5.5 mm)) for the region with $G' < 10^7$ Pa.

In the case of the shear sandwich measurements, the specimen was clamped between the plates and first heated

Table 2 Characteristics of blends

Sample code[a]	Moulding temperature (°C)[b]	Moulding time (min)[c]
PSAN20/PPE-II (80:20) m190	190	45
PSAN20/PPE-II (80:20) m210	210	45
PSAN20/PPE-II (80:20) m230	230	45
PSAN20/PPE-II (80:20) m250	250	180
PSAN43/PPE-I (60:40)	240	45
PSAN43/PPE-I/SM78 (60:40:10)	240	45
PSAN43/PPE-I/SM78 (60:40:20)	240	45
PSAN20/PPE-II (60:40)	240	45
PSAN20/PPE-II/SM78 (60:40:10)	240	45
PSAN20/PPE-II/SM78 (60:40:20)	240	45

[a] The weight ratio of the blend components is given in parentheses
[b] Temperature of the plates of the hydraulic press measured by a Pt thermocouple; accuracy in maintaining the desired temperature is ±3°C
[c] Time from placing the filled moulding forms between the hot plates till removal; the hot forms are rapidly cooled down with water; the effective time during which the sample has the moulding temperature is shorter, because of thermal lag of the moulding form

Table 1 Characteristics of polymers

Polymer	M_n[a] (kg mol^{-1})	M_w/M_n	w_S[b]	T_g D.s.c.[c]	T_g E''[d]	T_g tan δ[e]
SM78[j]	78;90[f]	1.17	0.47[g]	102;130	106;≈130[i]	110;135
PSAN20	160	1.6	0.89[h]	110	110	113
PSAN43	45	1.4	0.57[h]	111	114	116
PPE-I	43	1.53	0	215	216	227
PPE-II	90	2.0	0	215	216	227

[a] Combined results of g.p.c. and membrane osmosis
[b] Weight fraction PS
[c] Heating rate 10°C min^{-1}, inflection point method
[d] Maximum of E'' peak at 1 rad s^{-1}
[e] Maximum of tan δ peak at 1 rad s^{-1}
[f] First value corresponds to the PS block
[g] Determined from ^1H n.m.r.
[h] Determined from elemental analysis
[i] Shoulder on the high-temperature side of the E'' peak of PS
[j] SM78 is a poly(styrene-*b*-methyl methacrylate) diblock copolymer, number indicates molecular weight of the PS block

up to 240°C, where the screw of the plates was further tightened. At this temperature, strain sweep measurements with strains between 0.2 and 4% were performed until constancy of the mechanical response over this range of strains was achieved. This procedure ensures good mechanical contact between the sample and the plates. After that, the temperature was set to the desired initial temperature of the temperature-step test run. In the case of the samples PSAN20/PPE (80:20), which were prepared at different temperatures to demonstrate the influence of thermal history, the above procedure was performed at the corresponding moulding temperature of the samples.

Transmission electron microscopy

Ultrathin sections (≈50 nm) were cut at room temperature from the specimen tested with the dual cantilever tool with an ultramicrotome equipped with a diamond knife. Normally, the sections were taken from parts of the specimen where the test tool did not elongate the sample at the high temperatures at the end of the test run (i.e. temperatures in which $E' < 10^8$ Pa). In these parts the original morphology is preserved. Otherwise, sections from elongated parts showed some orientation (see *Figures 7b* and *7c*). Contrasting was performed by exposing the ultrathin sections on gold grids for 30 min to RuO_4 vapour according to the method of Trent *et al.*[32].

RESULTS AND DISCUSSION

Estimation of micelle formation tendency

Based upon the segmental interactions, we give a rough estimation in which of the bulk phases, PSAN or PPE, a symmetric block copolymer P(S-*b*-MMA) would have a higher tendency to form micelles. An exothermic heat of mixing is the basic requirement for miscibility between high-molecular-weight polymers[33]. The miscibility between PS and PPE originates from an exothermic mixing enthalpy expressed by a relatively large negative segmental interaction parameter $\chi_{S,PO} = -0.1$ (ref. 14).

The system PSAN/PMMA is an example of copolymer/homopolymer blends in which a small overall negative heat of mixing is explained by strong intrachain repulsion of styrene and acrylonitrile segments[18,19]. According to a simple mean-field binary interaction model[14,34,35], the interaction parameter $\chi_{PMMA,PSAN}$ can be expressed by the binary segmental interaction parameters appropriately weighted for copolymer composition, β being the mole fraction of styrene in PSAN:

$$\chi_{PMMA,PSAN} = \beta\chi_{MMA,S} + (1-\beta)\chi_{MMA,AN} - \beta(1-\beta)\chi_{S,AN} \quad (1)$$

with

$$\chi_{MMA,S} = 0.01 \qquad \chi_{MMA,AN} = 0.07 \qquad \chi_{S,AN} = 0.17$$

We took the χ parameters given by Kammer *et al.*[36] to calculate the effective interaction parameter $\chi_{PMMA,PSAN}$ for blends of PSAN20 ($\beta = 0.67$) and PSAN43 ($\beta = 0.40$) with PMMA. From equation (1) it follows that $\chi_{PMMA,PSAN20} \approx -0.008$ and $\chi_{PMMA,PSAN43} \approx +0.005$. These values represent rough estimates of the effective PMMA/PSAN interaction parameters without considering any detailed temperature or concentration dependence of the segmental interactions, because this is not within the scope of the model leading to equation (1). Despite the lack of exact numerical values, it may be concluded that in ternary blends at moulding temperatures in the region of 240°C the interaction of the PS blocks with the PPE phase is much more favourable than the interaction of the PMMA blocks with the PSAN20 phase (and all other PSAN copolymers miscible with PMMA). Based on analogous relations to those of equation (1), the segmental interaction parameters between PMMA and PPE, $\chi_{MMA,PO}$, and between polyacrylonitrile and PPE, $\chi_{AN,PO}$, were estimated from the miscibility limits of P(S-*co*-MMA) with PPE and P(S-*co*-AN) with PPE: $\chi_{MMA,PO} \approx 0.5$ (ref. 37), $\chi_{AN,PO} \approx 0.5$ (ref. 16), i.e. very unfavourable. In analogy to equation (1) the effective interaction parameters for binary blends of PSAN20 and PSAN43 with PPE can be calculated: $\chi_{PPE,PSAN20} \approx 0.06$, $\chi_{PPE,PSAN43} \approx 0.22$.

Concerning the behaviour of P(S-*b*-MMA) in ternary blends with PSAN and PPE, the different enthalpic contributions will decisively determine the location of the block copolymer, i.e. whether or not micelles will be formed and in which of the bulk phases micelle formation is more likely to occur (*Figure 1*). In ternary blends of PPE, P(S-*b*-MMA) and PSAN with compositions in the centre of the PSAN/PMMA miscibility window (i.e. PSAN15–PSAN25), the block copolymer should have a strong tendency to locate at the interface, because in such an arrangement both blocks can mix exothermally with the respective blend components. Along the same arguments the *CMC* should be higher in such an A/C-D/B system compared to an A/A-B/B system. Nevertheless, at higher concentrations of the block copolymer, micelles may be formed. In a ternary blend with approximately equal amounts of PSAN20 and PPE, both of similar molar mass, a symmetric P(S-*b*-MMA) block copolymer is expected to form micelles in the PPE phase, rather than in the PSAN20 phase. The obvious thermodynamic explanation is that in such an arrangement the much stronger favourable interaction between the PS segments and PPE is preserved, at the expense of the less favourable interaction between the PMMA segments and PSAN20.

Influence of preparation conditions on the dynamic mechanical and morphological properties — how to choose the best sample preparation

For investigations on the miscibility behaviour of polymer blends, it is always desirable to deal with systems in equilibrium states, or as close to equilibrium as possible. Nevertheless, owing to the high viscosities in high-molecular-weight systems this is often not the case, especially under industrial blending conditions. Laboratory-scale blend preparation usually involves solution methods like casting or coprecipitation. In the case of PSAN/PPE/P(S-*b*-MMA) we are dealing with a system having four different polymer components with different solubility characteristics. Therefore, it is impossible to find a non-selective solvent that would allow blend preparation by casting without interfering solvent effects[38]. Moreover, casting from solution leads to crystallization of the PPE[39]. We chose the method of coprecipitation from dilute solution into a large excess of non-solvent as a method of producing an intimate mixture of the components. According to the dynamic

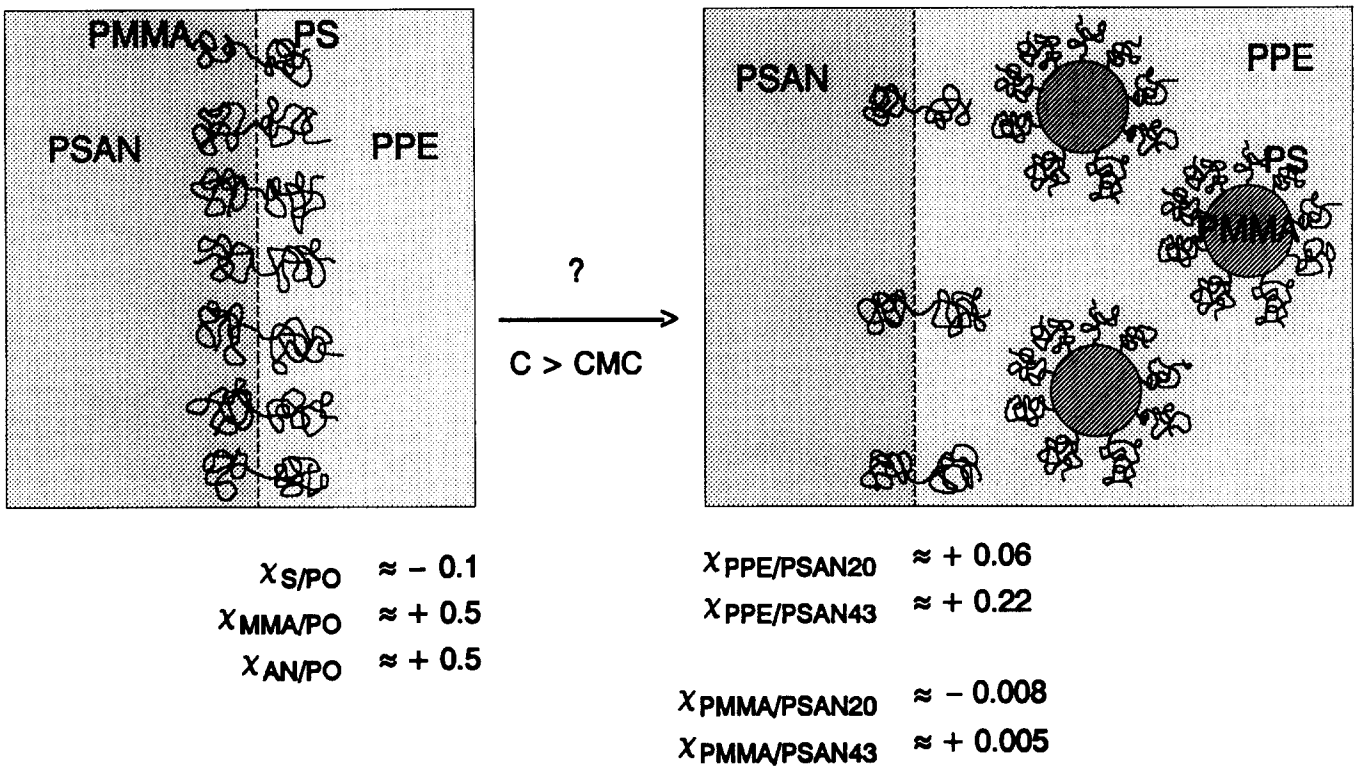

Figure 1 Schematic diagram of the interfacial situation in ternary blends PSAN/PPE/P(S-*b*-MMA) with an estimation of the interactions according to χ parameters. The possibility that block copolymers could dissolve homogeneously in the bulk phases has been neglected, owing to the high molecular weight of all components

mechanical analysis this method avoids crystallization of the PPE phase*.

The dried powders are used to prepare samples by melt pressing. As will be shown below, the extremely fine dispersion prepared in this manner is a good starting point in order to prepare samples close to an equilibrium state. The melting temperature should be significantly higher than the glass transition temperature of PPE (215°C, d.s.c., 10°C min^{-1}), but is limited by the stability of the PMMA block.

In previous experiments we examined the influence of moulding temperature on the molecular-weight distribution of the pure block copolymer SM78[24]. It was found that, in the temperature range between 230 and 250°C (45 min, vacuum), the degree of degradation is very low and still acceptable. At 230°C the polydispersity increased from $M_w/M_n = 1.09$ to 1.18 and M_w was reduced by 8%; at 250°C, however, M_w/M_n already increased to 1.29, while M_w decreased by 27%.

The influence of the thermal history on dynamic mechanical and morphological properties was investigated in a binary blend of PSAN20/PPE-II (80:20). For blends of this composition the dynamic mechanical behaviour can be tested with the shear sandwich from above the PSAN20 glass transition (i.e. above ≈125°C) up to temperatures well above the PPE glass transition.

Figure 2a shows the G' data from samples that were prepared at different moulding temperatures. All samples were transparent because PSAN20 and PPE have similar refractive indices. The samples that were melt pressed at 190 and 210°C, i.e. at temperatures below the PPE glass transition (PSAN20/PPE-II (80:20) m190 and PSAN20/PPE-II (80:20) m210), show a gradual decrease in modulus in the region between the two glass transitions. Such behaviour is characteristic for highly dispersed systems with broad interfacial regions, where the different chains are intermixed[44–46]. In these blends this situation is caused by the rapid precipitation process from dilute solution and the inability of the highly dispersed PPE phase to coalesce at melting temperatures below the T_g of PPE. At higher temperatures above the T_g of PPE the phase separation process continues and leads to coarsening of the phases. Accordingly, in the case of the sample kept at 250°C for 180 min (PSAN20/PPE-II (80:20) m250) the modulus between the two glass transitions remains constant with a sharp drop at the PPE glass transition. Such a behaviour is typical for grossly phase-separated systems with sharp interfaces[44–46].

Figure 2b shows the corresponding variation of tan δ in going from the highly dispersed system with strong phase intermixing to the coarsely phase-separated structure with narrow interface. The samples prepared at 190 and 210°C show the relaxation of the broad interphase as an asymmetric broadening of the tan δ peak to lower temperatures (curves C and D in *Figure 2b*). A strong sharpening of the tan δ maximum is observed for the sample prepared at 230°C and even more pronounced at 250°C (curves A and B in *Figure 2b*). It is important to note that in these samples the maximum of the PPE

* Depending on sample characteristics, semicrystalline PPE shows an endotherm melting transition in the range ≈235–260°C[40]. PPE that is cooled from the melt has little measurable crystallinity[41]. However, in the presence of solvents[42] or solvent vapours[43], crystallization easily takes place. Ternary blends PSAN20/PPE/P(S-*b*-MMA) (80:20:5) that were cast from $CHCl_3$ solution revealed crystallinity according to the dynamic mechanical analysis. The relaxation of crystalline domains overlaps the PPE glass transition. Therefore, samples with semicrystalline PPE show a broadening of the tan δ peak of the PPE glass transition to higher temperatures. Heating the samples above ≈250°C irreversibly removes crystallinity. In precipitated and subsequently melt-pressed samples (240°C), this behaviour is not found, indicating that no significant crystallinity is present

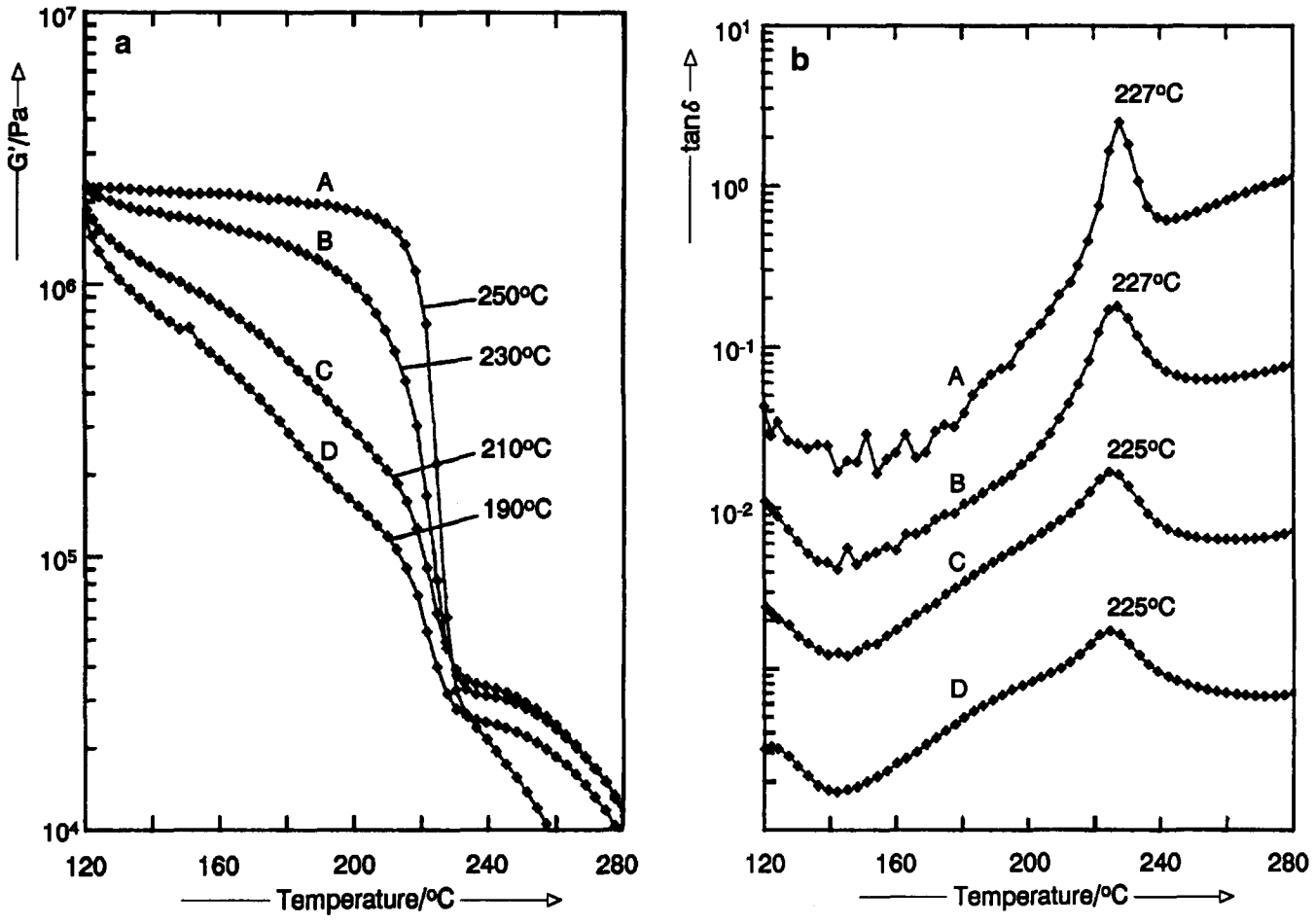

Figure 2 Influence of thermal history on dynamic mechanical properties of a binary blend PSAN20/PPE-II (80:20). Samples: (A) PSAN20/PPE-II (80:20) m250, (B) PSAN20/PPE-II (80:20) m230, (C) PSAN20/PPE-II (80:20) m210, (D) PSAN20/PPE-II (80:20) m190. (a) G' data from testing with shear sandwich. The 190, 210 and 230°C samples were melt pressed for 45 min, the 250°C sample for 180 min. (b) For better comparison the corresponding tan δ curves are vertically offset against each other by one decade. The correct ordinate scale refers to the upper curve

tan δ peak does not shift significantly and the temperature of 227°C corresponds to the value in pure PPE. This means that all samples are phase-separated with a dispersed phase consisting mainly of pure PPE. The fraction of intermixed material, which is rather high owing to the coprecipitation technique, strongly reduces at moulding temperatures above 220°C. This interpretation of d.m.a. data can be checked by electron microscopy.

Figures 3a–c show the TEM micrographs of the samples prepared at 190 and 250°C. As expected from the mechanical behaviour, the sample prepared at 190°C displays an extremely fine dispersed morphology, in which small PPE particles are randomly embedded in the PSAN20 matrix (*Figure 3a*). Most of the particles are spherical in shape with diameters less than $\approx$50 nm. *Figures 3b* and *3c* show the same blend prepared at 250°C. The PPE phase has significantly coarsened to large irregular-shaped particles. Most of them have dimensions in the range $\approx$0.5–1 μm. There are also smaller structures looking like small isolated PPE particles or inclusions of PSAN in PPE, but this feature most probably arises from preparing ultrathin sections ($\approx$50 nm), thus cutting through the edges of larger irregular-shaped structures.

The coarsening of the PPE phase from the state in *Figure 3a* to that in *Figures 3b* and *3c* is a process based only on diffusion, because no shearing forces were applied to the melt. Owing to the high viscosity in the temperature range between 230 and 250°C, the coarsening process is rather slow and leads to irregular-shaped structures according the shortest diffusion paths. The addition of P(S-*b*-MMA) reduces the melt viscosities in this temperature range, because the T_g of both blocks are much lower. With these experiments it has been demonstrated that melt pressing the precipitated highly dispersed material of ternary blends PSAN/PPE/P(S-*b*-MMA) at 240°C avoids damaging the PMMA block and will produce samples that have approached equilibrium, suitable for studying the basic effects of the block copolymers.

Contrast in TEM

Thin sections of unstained blends of PSAN20 and PPE do not give sufficient scattering contrast in TEM. The familiar staining method with OsO_4 cannot be applied, because olefinic unsaturation or other reactive groups are not present in one of the phases. The much more reactive RuO_4 also attacks aromatic unsaturation. Therefore it can be used to stain PSAN/PPE blends.

Trent *et al.*[32] have demonstrated that RuO_4 readily stains PS, PSAN and PPE, whereas PAN and PMMA do not react. Thus, increasing the AN content in PSAN will reduce the reactivity towards RuO_4. Indeed, in blends of PSAN43 with PPE we gained excellent contrast: the PPE domains were considerably stained (see *Figures 5a–c*). In the case of PSAN20 and PPE the reactivities towards RuO_4 are very similar and the phases are stained to approximately equal degree. Fortunately

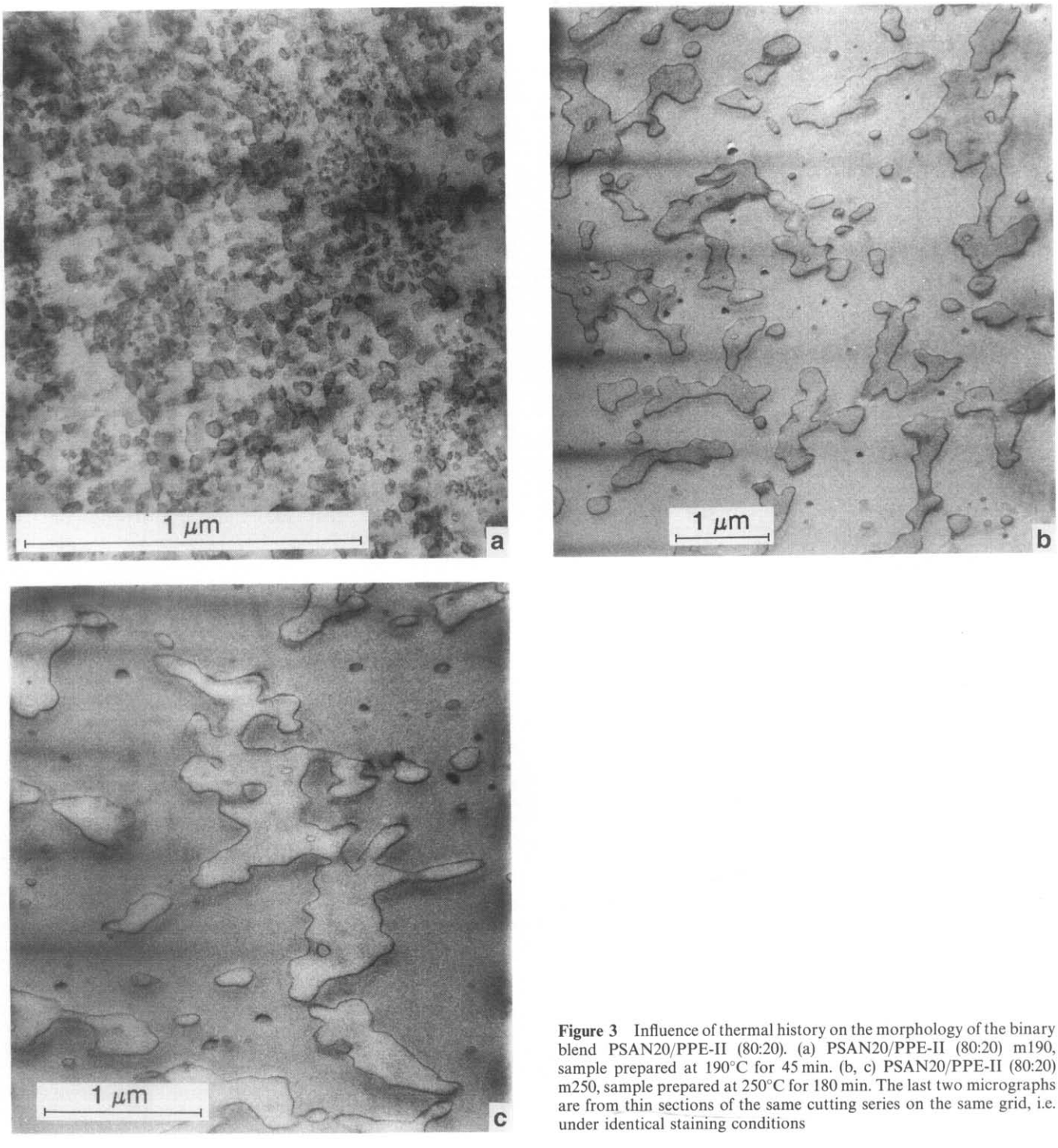

Figure 3 Influence of thermal history on the morphology of the binary blend PSAN20/PPE-II (80:20). (a) PSAN20/PPE-II (80:20) m190, sample prepared at 190°C for 45 min. (b, c) PSAN20/PPE-II (80:20) m250, sample prepared at 250°C for 180 min. The last two micrographs are from thin sections of the same cutting series on the same grid, i.e. under identical staining conditions

the phase boundaries are obviously attacked much faster by RuO_4, therefore clearly indicating the contours of the particles (*Figures 3a–c*). In blends with technical PPE with relative large amount of phenolic chain end-groups, which are probably more reactive towards RuO_4, the staining situation may be different. Depending on sample history, staining conditions and TEM operation, in some cases a weak contrast between the bulk phases of PSAN20 and PPE developed.

As shown in *Figure 3a* in the case of the partially demixed blend PSAN20/PPE-II (80:20) m190, the PPE phase was more strongly stained. *Figures 3b* and *3c* show micrographs obtained from the 250°C sample on the same grid, i.e. under identical staining conditions. In micrograph *3b*, the PPE phase appears slightly darker, whereas in micrograph *3c* the situation is reversed. As a consequence, in blends with comparable amounts of PSAN20 and PPE, a correct assignment of the components to the domains may become difficult.

Dynamic mechanical and morphological behaviour of ternary blends PSAN43/PPE/P(S-b-MMA)

Figures 4a–c compare the dynamic mechanical behaviour of blends PSAN43/PPE-I (60:40) with varying amounts of the block copolymer SM78. To cover the mechanical behaviour over both glass transitions, each sample was tested with two testing geometries (see 'Experimental' section). In the temperature range of high moduli, i.e. in these blends up to the glass transition of the PPE phase,

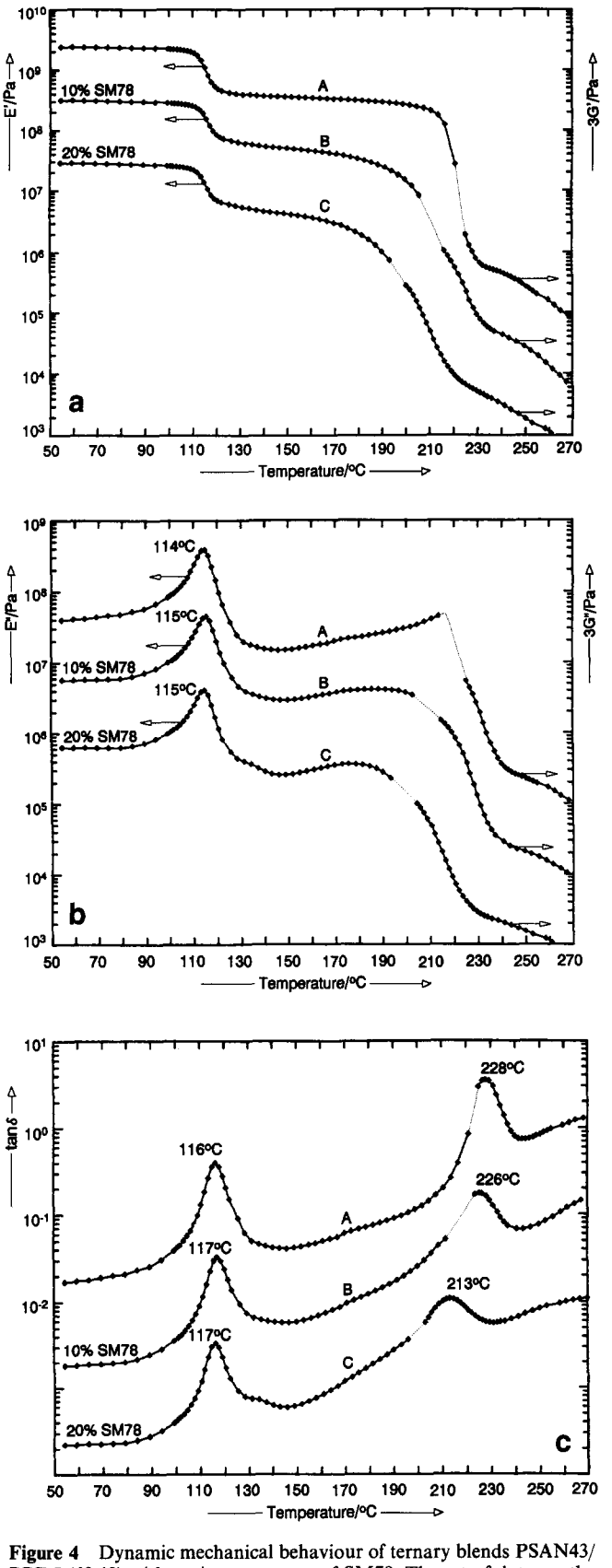

Figure 4 Dynamic mechanical behaviour of ternary blends PSAN43/PPE-I (60:40) with various amounts of SM78. The set of data on the left correspond to measurements with the dual cantilever fixture, the set of data on the right to measurements with the shear sandwich fixture. Curves of the different blends are vertically offset against each other by one decade. The correct ordinate scale always refers to the uppermost curve A of the binary blend without block copolymer. Samples: (A) PSAN43/PPE-I/SM78 (60:40:0), (B) PSAN43/PPE-I/SM78 (60:40:10), (C) PSAN43/PPE-I/SM78 (60:40:20). (a) Temperature variation of storage modulus; G' data are offset by a factor of 3. (b) Temperature variation of loss modulus; G'' data are offset by a factor of 3. (c) Temperature variation of tan δ

the dual cantilever geometry was used, whereas for higher temperatures the shear sandwich geometry was applied. Young's modulus data as well as shear modulus data are represented together. For direct comparison the shear modulus data are offset by a factor of 3, according to[47] $E=2(1+\nu)G$, assuming incompressible behaviour in the melt with a Poisson ratio of $\nu=0.5$, which is a reasonable approximation. Between the two sets of data a small gap always remained, where no reliable data could be obtained, but this does not restrict the overall analysis and conclusions.

Upon addition of P(S-*b*-MMA) to PSAN43/PPE (60:40) blends the PPE glass transition is shifted to lower temperatures and becomes broader (*Figures 4a–c*). The maximum of the tan δ peak is shifted from 228°C in the binary blend PSAN43/PPE-I (60:40) (curve A in *Figure 4c*) to 226 and 213°C in ternary blends with 10% and 20% P(S-*b*-MMA) (curves B and C). Owing to the immiscibility of PSAN43 and PMMA, the block copolymer forms micelles in the PPE phase with a PMMA core. Starting from the surface of PMMA micelle cores, the PS chains extend into the PPE phase. The influence on the PPE glass transition depends on the distribution of PS and PPE segments. In parallel experiments we demonstrated that P(S-*b*-MMA) of various molar masses does not show homogeneous solubility in high-molecular-weight PPE[48]. If large portions of the PPE phase are penetrated by the PS blocks, the glass transition will be broadened and shifted to lower temperatures. The experiments show that this effect increases at higher concentrations of P(S-*b*-MMA). In contrast to the PPE glass transition, the glass transition of PSAN43 is not altered according to the E'' and tan δ analysis in *Figures 4b* and *4c*, neither in temperature nor in width (*Table 3*). The highly syndiotactic PMMA block has a T_g of 130°C (d.s.c., 10°C min^{-1}), leading to a maximum in tan δ at 135°C (1 rad s^{-1}) in the dynamic mechanical analysis. At a block copolymer concentration of 20% the glass transition of the micellar PMMA cores can be clearly detected as a shoulder on the high-temperature side of the PSAN43 E'' and tan δ peak (curves C in *Figures 4b* and *4c*). At a level of 10% P(S-*b*-MMA) this transition is covered by overlapping of the stronger PSAN43 glass transition (curves B in *Figures 4b* and *4c*). The turbid appearance of all blends with PSAN43 proves their coarsely separated structure.

Table 3 Dynamic mechanical characterization of the glass transition of the PSAN phase in the different blends

	E'' peak		tan δ peak	
SM78 (wt%)	T (°C)	Peak width (°C)[a]	T (°C)	Peak width (°C)[b]
Blends PSAN20/PPE-II (60:40)				
0	110	9.8	112	9.1
10	111	10.1	113	9.8
20	112	10.6	115	10.6
Blends PSAN43/PPE-I (60:40)				
0	114	8.1	116	8.1
10	115	7.6	117	8.3
20	115	8.1	117	8.1

[a] Width of the E'' peak at half-height, drawing an arbitrary baseline parallel to the temperature abscissa through the E'' value at 50°C
[b] Half-height width of the tan δ peak, drawing the baseline as the tangent, connecting the beginning and the end of the tan δ peak

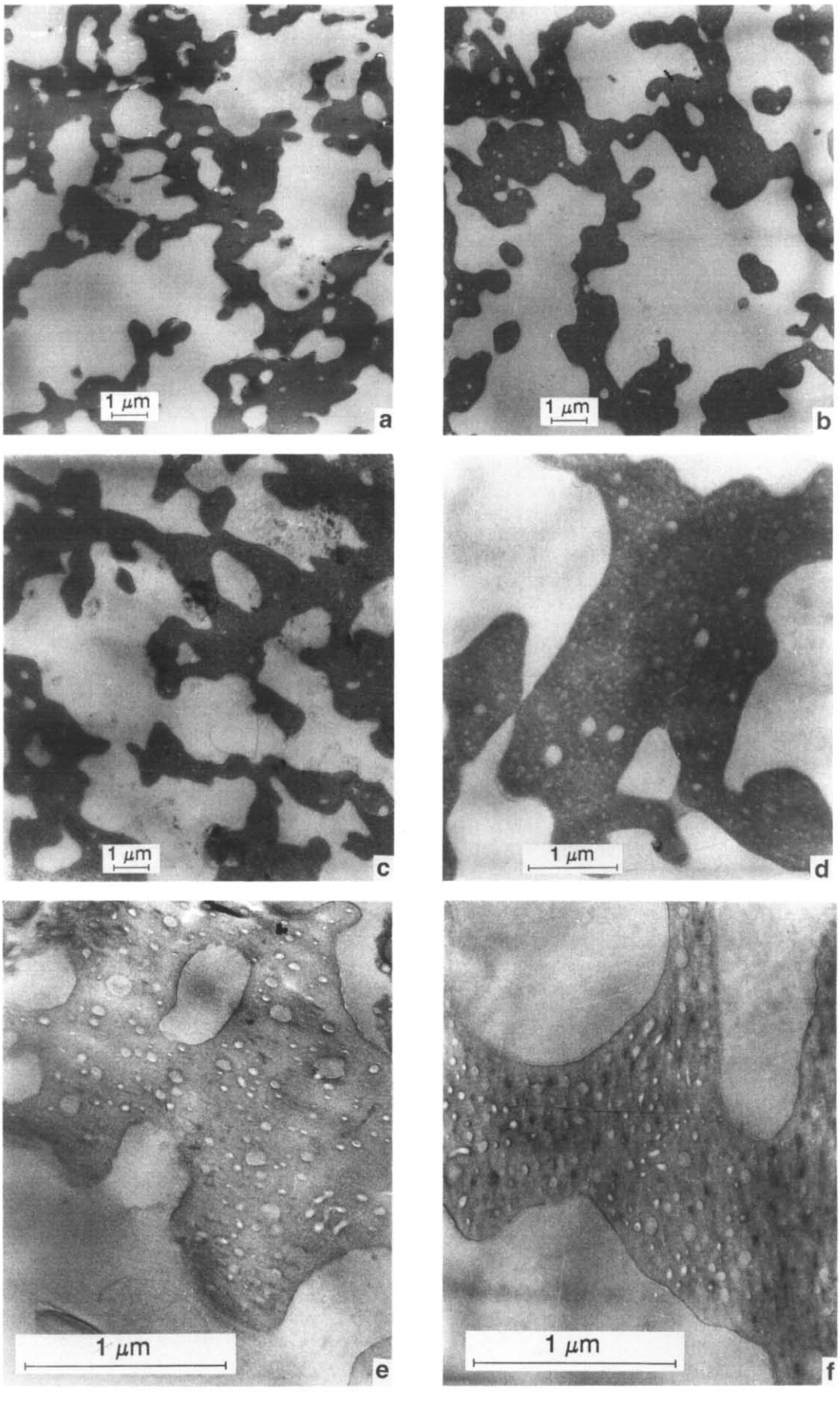

Figure 5 Morphology of blends PSAN43/PPE-I (60:40) with various amounts of the block copolymer SM78. (a)–(c) Low magnification showing large-scale morphology: (a) binary blend without block copolymer, PSAN43/PPE-I (60:40); (b, c) ternary blends, (b) PSAN43/PPE-I/SM78 (60:40:10), (c) PSAN43/PPE-I/SM78 (60:40:20). (d) Stronger magnification of the blend PSAN43/PPE-I/SM78 (60:40:10) showing some inclusions of PSAN43 ($\approx$100–200 nm) and diffuse small PMMA cores of the micelles, which cover the whole PPE-phase. (e, f) Stronger magnifications of parts of the PPE-phase: (e) blend PSAN43/PPE-I/SM78 (60:40:10); (f) blend PSAN43/PPE-I/SM78 (60:40:20)

The TEM analysis of these blends is shown in *Figures 5a–e*. As seen from *Figures 5a–c* (low magnifications), addition of P(S-*b*-MMA) does not cause alterations in the large-scale morphology. The blends show a coarse phase-separated morphology with irregular-shaped PPE domains with a relative high degree of connectivity and dimensions well above 1 μm. Thus, in blends with PSAN43 the P(S-*b*-MMA) block copolymer has no dispersing efficiency. At higher magnifications (*Figures 5d* and *5e*), the block copolymer micelles are clearly detected in the PPE phase, because the PMMA core is not stained. Spherical micelles are homogeneously distributed over the whole PPE phase with an apparent core diameter ranging from $\approx$20 to 40 nm. In addition, some larger structures are observed with diameters of the order 50–200 nm. These are most probably inclusions of PSAN43 in PPE. The micelles show no tendency for preferential segregation to the PSAN43/PPE phase boundary, as reported for other systems[49,50]. As can be seen from the micrographs *5e* and *5f*, a regime extending approximately 20 nm from the phase boundary is essentially free from micelle cores. Enhancing the concentration of P(S-*b*-MMA) from 10% (*Figures 5d* and *5e*) to 20% (*Figure 5f*) increases the number of micelles, but the core dimensions remain unaffected. This observation is in agreement with the dynamic mechanical behaviour. Owing to the smaller number of micelles in the blend with 10% P(S-*b*-MMA), the average distance between neighbouring micelles is larger. Therefore the amount of PPE that is penetrated by the PS blocks is rather low. Correspondingly, the location of the PPE glass transition is only slightly lowered by 2°C (curve B in *Figure 4c*). At a level of 20% P(S-*b*-MMA) the average distance between the larger number of micelles is smaller and significant amounts of the PPE phase are penetrated by the PS blocks. Thus the maximum of tan δ is lowered to 207°C (curve C in *Figure 4c*). On all micrographs the PSAN43 phase appears uniform with no indication of micelle formation or macrophase separation of P(S-*b*-MMA). Owing to the higher reactivity of PS microdomains towards RuO_4 compared to PSAN43, this would be easily detectable.

Mechanical and morphological behaviour of blends PSAN20/PPE/P(S-b-MMA)

Blends of PSAN20/PPE (60:40) with different amounts of P(S-*b*-MMA) show completely different behaviour (*Figures 6a–c*). The lowering of the glass transition of the PPE phase by the addition of P(S-*b*-MMA) is much more pronounced than in the corresponding PSAN43 blends. The maximum of tan δ is reduced from 227°C in the binary blend PSAN20/PPE-II (60:40) (curve A in *Figure 6c*) to 219 and 207°C in ternary blends with 10% and 20% P(S-*b*-MMA) (curves B and C in *Figure 6c*). Owing to the miscibility of PSAN20 and PMMA, in these blends the block copolymer is completely located at the interface, with the PS blocks extending into the highly dispersed PPE phase. In the blend with 20% P(S-*b*-MMA), the curves of E'' and tan δ do not indicate a glass transition of PMMA microdomains on the high-temperature side of the corresponding peak of the PSAN20 glass transition (curves B and C in *Figures 6b* and *6c*). Thus, no micelle formation is detectable in the d.m.a. experiment. Moreover a slight increase of the PSAN20 transition is observed. Though the high-temperature transition is rather broad, reflecting a distribution of PS/PPE

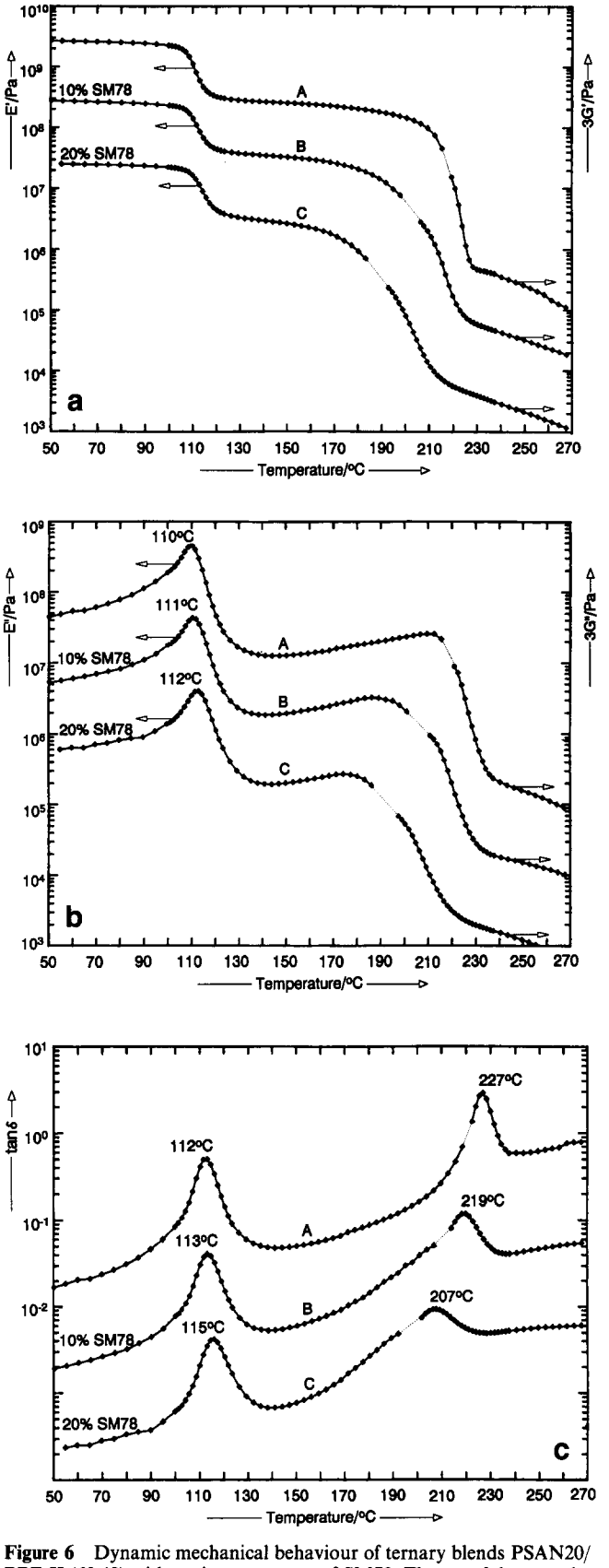

Figure 6 Dynamic mechanical behaviour of ternary blends PSAN20/PPE-II (60:40) with various amounts of SM78. The set of data on the left correspond to measurements with the dual cantilever fixture, the set of data on the right to measurements with the shear sandwich fixture. Curves of the different blends are vertically offset against each other by one decade. The correct ordinate scale always refers to the uppermost curve A of the binary blend without block copolymer. Samples: (A) PSAN20/PPE-II (60:40), (B) PSAN20/PPE-II/SM78 (60:40:10), (C) PSAN20/PPE-II/SM78 (60:40:20). (a) Temperature variation of storage modulus; G' data are offset by a factor of 3. (b) Temperature variation of loss modulus; G'' data are offset by a factor of 3. (c) Temperature variation of tan δ

compositions, the maximum of tan δ is strongly shifted to lower temperatures upon addition of P(S-*b*-MMA). In these blends the mixing of the PS blocks with PPE apparently is more homogeneous than in the corresponding PSAN43 blends, where the block copolymer forms micelles in the coarse grain structure of the PPE phase.

The T_g of the PPE/PS mixed phase can be compared with that of binary PS/PPE blends of similar composition, in which T_g varies with composition according to the Gordon–Taylor equation[51]. For the compositions PS block/PPE of 5:40 and 10:40 in the ternary blends with PSAN and PPE, the reduction of T_g can be estimated, taking the temperature at the maximum of the tan δ peak as T_g value (PPE, 227°C; PS, 110°C; Gordon–Taylor constant $K = 0.79$[51]). In the case of an unrestricted mixing of PS blocks with PPE, T_g of the mixed PS/PPE phase is expected to be 211 and 199°C for ternary blends with 10% and 20% P(S-*b*-MMA) respectively, i.e. if complete homogeneous interpenetration of PPE and PS segments occurs. These values are clearly not reached in the ternary blends PSAN20/PPE-II/SM78 (60:40:10) and PSAN20/PPE-II/SM78 (60:40:20) (219 and 207°C respectively, *Figure 6c*). This indicates that the composition varies across the PPE/PS phase. The PS segment density decreases from high values near the interface to low values in the inner regions of the PPE phase. This causes a strong broadening of the PS/PPE glass transition as compared to homogeneous binary blends of PS/PPE, where only little broadening of the glass transition is observed.

The temperature of the maximum of tan δ will approximately correspond to compositions that are most frequently present. The addition of P(S-*b*-MMA) causes only slight alterations of the PSAN20 glass transition. *Table 3* summarizes the glass transition data obtained from dynamic mechanical analysis of the PSAN glass transition in the different blends. Upon the addition of P(S-*b*-MMA), in blends with PSAN20 a very slight increase in temperature and width of the E'' and tan δ peak of the PSAN20 glass transition is observed. The alterations on the PSAN20 glass transition due to mixing of PSAN20 with PMMA blocks are small, because the difference in T_g between PSAN20 (tan $\delta_{max} = 113$°C) and PMMA (tan $\delta_{max} = 135$°C) amounts to only ≈ 22°C.

Taking the temperature of the maximum of tan δ (*Table 1*) as a measure of T_g, one can estimate this temperature shift for the most extreme case where PSAN20 and PMMA blocks are uniformly mixed. The temperature dependence of T_g on composition in binary blends of PSAN20 and PMMA deviates from linearity in the sense that T_g is slightly lower than expected. Therefore the linear correlation can be taken as an upper limit for the T_g shift of the PSAN20 glass transition upon mixing with the PMMA blocks. For the blend PSAN20/PPE (60:40) with 20% SM78 the weight ratio of PSAN20 to PMMA blocks is 60:10. The glass transition of a corresponding binary blend of PSAN20 and PMMA can be estimated to be 116°C assuming a linear T_g–composition relation. In the case of a slight negative deviation from linearity, it would be less. As can be seen from *Figures 6b* and *6c* and *Table 3* this weak shift in the range of 2–3°C is indeed observed, accompanied by a corresponding slight increase in half-height width of the E'' and tan δ peak. In these blends with high weight ratios of PSAN20 to PMMA blocks, the alterations on the PSAN20 glass transition were found to be very small, as expected. Therefore the dynamic mechanical behaviour is in full accordance with the interpretation that the block copolymers stick to the interface in a wet-brush situation with significant mixing of PMMA blocks with PSAN20 and, respectively, PS blocks with PPE.

The TEM micrographs of the blends with 10% and 20% P(S-*b*-MMA) demonstrate the compatibilizing efficiency of the block copolymer SM78 (*Figure 7c*). As described in the section above, the contrast between PSAN20 and PPE is weak, but the contour lines of the phases are clearly visible. In micrographs *7a*, *7b* and *7c* the PPE phase appears slightly more strongly stained. The PPE phase is finely dispersed, irregularly shaped with a high degree of connectivity. Enhancing the amount of P(S-*b*-MMA) from 10 to 20% further improves dispersion. *Figure 7c* gives a micrograph of the blend with 20% SM78 at a higher resolution. In both phases there are no indications of a fine structure resulting from micelle formation of the block copolymer. Thus the electron micrographs give the same results as the dynamic mechanical analysis. No micelles are detectable.

The thin section for the micrograph in *Figures 7b* and *7c* was cut from a part of the dual cantilever specimen, where at high temperatures the test tool deformed the sample. Therefore the structure shows some anisotropy. The domains of the PPE phase in the micrographs in *Figure 7* have shortest diameters in the range ≈ 50–100 nm. This high degree of dispersion is a basic requirement for the validity of the above picture, developed from the d.m.a. analysis. Phase dimensions have to be comparable with block copolymer dimensions to explain the observed strong influence on T_g of the PPE-rich phase. The PS block with $M_n = 78\,000$ has an unperturbed radius of gyration of $R_G^\circ = 7.7$ nm*. Starting from the block copolymer joint, which is located at the phase boundary, the PS blocks extend into the PPE phase. Large portions of the PPE are intermixed with PS blocks. Probably the strong enthalpic driving force of the PS–PPE interaction leads to considerable stretching of the PS chains[52], which are arranged in the form of a 'wet polymer brush'[8] at the interface. In accordance with this picture, the alteration of the PPE glass transition strongly depends on molecular weight and chemical composition of the block copolymer[53].

CONCLUSION

It has been demonstrated by dynamic mechanical spectroscopy and TEM that block copolymers P(S-*b*-MMA) display strong compatibilizing efficiency in the sense of a dispersing effect in ternary blends with PSAN20 and PPE. The P(S-*b*-MMA) is completely located at the interface within experimental accuracy. In combination with small dimensions of the PPE phase a significant temperature reduction of T_g of PPE is observed. Even at concentrations of P(S-*b*-MMA) as high as 20%, no micelle formation occurs. This behaviour can be compared with systems A/A-B/B, in which the blocks of the compatibilizer are chemically identical with the component phases. In such systems, depending on the molecular characteristics of the components, the *CMC*

* Calculated according to $\langle R_G^\circ \rangle^2 = \frac{1}{6} C^\infty N l^2$ with $N = 2M/M_0$, characteristic ratio $C^\infty = 10$, $l = 0.154$ nm, $M = 78\,000$, $M_0 = 104$

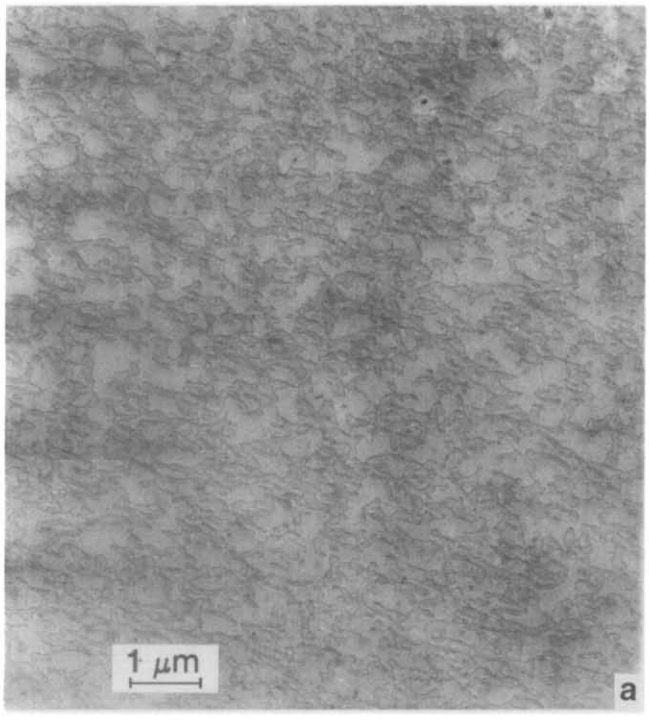

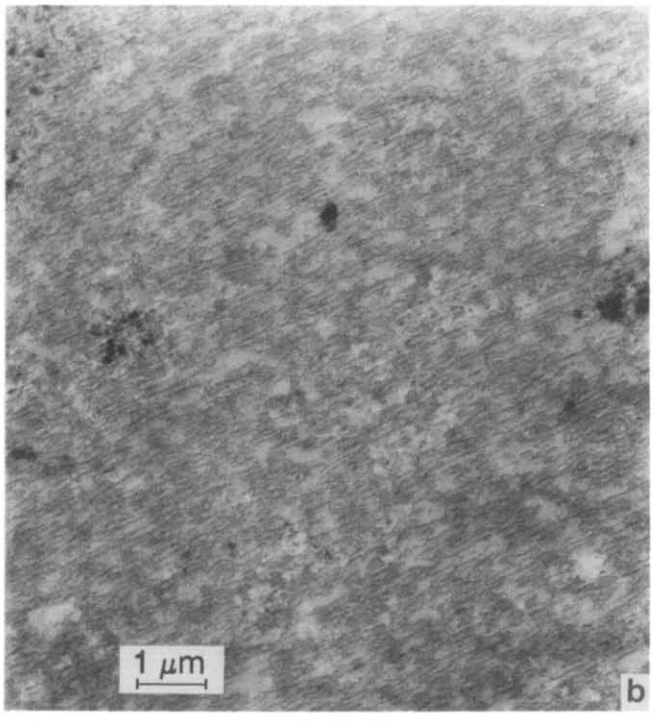

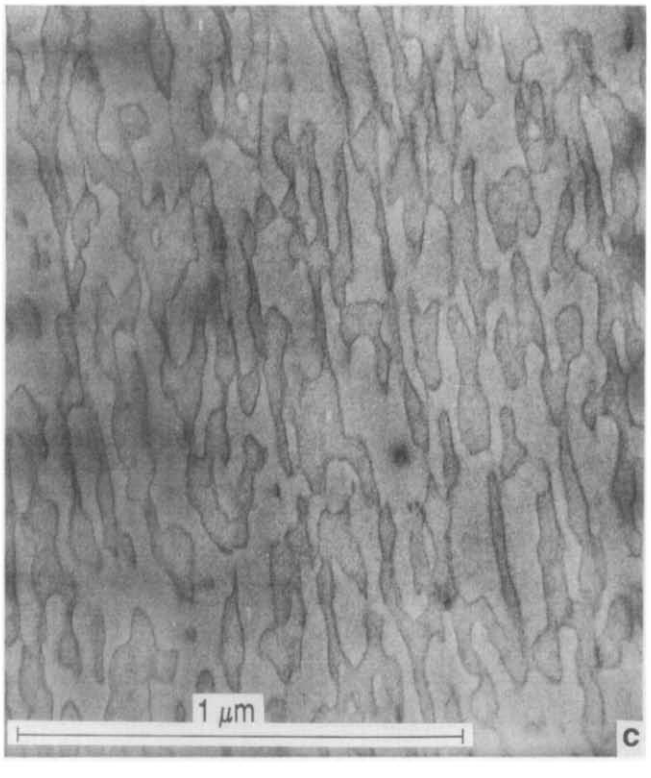

Figure 7 Morphology of ternary blends: (a) blend PSAN20/PPE-II/SM78 (60:40:10); (b) blend PSAN20/PPE-II/SM78 (60:40:20); (c) higher magnification of the same blend as (b)

was found to be typically in the range of only a few per cent by weight of block copolymer[5,6,49]. We conclude that in systems A/C-D/B with favourable exothermic heat of mixing between the blocks of the compatibilizer and the corresponding phases, the affinity of the block copolymer to both components is responsible for its preferential location at the blend phase boundary. Micelle formation is suppressed up to high concentrations, especially for all concentration ranges of practical importance. In contrast to this, in blends of PSAN43 and PPE, P(S-*b*-MMA) has no dispersing efficiency at all. Owing to the immiscibility of PSAN43 and the PMMA block, P(S-*b*-MMA) only forms spherical micelles in the PPE phase, with no indication of a preferential location at the phase boundary. In binary blends without block copolymer the effect of preparation conditions on the dynamic mechanical and morphological behaviour was examined in detail. This was done to establish preparation conditions under which the blends approach equilibrium without thermal degradation of P(S-*b*-MMA).

ACKNOWLEDGEMENTS

We are very grateful to Dr K. Mühlbach (BASF, Ludwigshafen) for fruitful discussions and supply of PSAN samples and to Dr W. Heckmann (BASF,

Ludwigshafen) for helpful suggestions concerning staining procedure. We are also very much indebted to Mr R. Würfel for careful operation of the EM. Financial support from BMFT and BASF through project 03 M 4041 is gratefully acknowledged.

REFERENCES

1 Paul, D. R. 'Polymer Blends', Academic Press, New York, 1978, Vol. 2, Ch. 12
2 Teyssie, Ph., Fayt, R. and Jerome, R. *Makromol. Chem., Macromol. Symp.* 1988, **16**, 41
3 Paul, D. R. 'Thermoplastic Elastomers. A Comprehensive Review' (Eds. N. R. Legge, G. Holden and H. E. Schroeder) Hanser, Munich, 1987, Ch. 12/6
4 Russel, T. P., Anastasiadis, S. H., Menelle, A., Felcher, G. P. and Satija, S. K. *Macromolecules* 1991, **24**, 1575
5 Noolandi, J. and Hong, K. M. *Macromolecules* 1982, **15**, 482
6 Anastasiadis, S. H., Gancarz, I. and Koberstein, J. T. *Macromolecules* 1989, **22**, 1449
7 Noolandi, J. and Hong, K. M. *Macromolecules* 1984, **17**, 1531
8 Leibler, L. *Makromol. Chem., Macromol. Symp.* 1988, **16**, 1
9 Shull, K. R. and Kramer, E. J. *Macromolecules* 1990, **23**, 4769
10 Schwarz, M. C., Keskkula, H., Barlow, J. W. and Paul, D. R. *J. Appl. Polym. Sci.* 1988, **35**, 653
11 Heuschen, J., Vion, J. M., Jerome, R. and Teyssie, Ph. *Polymer* 1990, **31**, 1473
12 Ouhadi, T., Fayt, R., Jerome, R. and Teyssie, Ph. *J. Polym. Sci. (B) Polym. Phys* 1986, **24**, 973
13 Schultz, A. R. and Gendron, B. M. *J. Appl. Polym. Sci.* 1972, **16**, 461
14 Kambour, R. P., Bendler, J. T. and Bopp, R. C. *Macromolecules* 1983, **16**, 753
15 Alexandrovich, P., Karasz, F. E. and MacKnight, W. J. *J. Appl. Phys.* 1976, **47**, 425
16 Kressler, J. and Kammer, H. W. *Acta Polym.* 1987, **38**, 600
17 Stein, D. J., Jung, R. H., Illers, K. H. and Hendus, H. *Angew. Makromol. Chem.* 1974, **36**, 89
18 Suess, M., Kressler, J. and Kammer, H. W. *Polymer* 1987, **28**, 957
19 Fowler, M. E., Barlow, J. W. and Paul, D. R. *Polymer* 1987, **28**, 1177
20 Won, J. H., Kim, H. C. and Baik, D. H. *Macromolecules* 1991, **24**, 2231
21 Mylonakis *et al.*, US Patent 4866126, 1989
22 Fetters, L. J. and Morton, M. *Macromol. Synth.* 1972, **4**, 77
23 Allen, R. D., Long, T. E. and McGrath, J. E. *Polym. Bull.* 1986, **15**, 127
24 Auschra, C. and Stadler, R. *Polym. Bull.* in press
25 Percec, V. and Shaffer, T. D. *J. Polym. Sci., Polym. Lett. Edn.* 1986, **24**, 439
26 Bruice, T. C., Kharash, N. and Winzler, R. J. *J. Org. Chem.* 1953, **18**, 83
27 White, D. M. *Polym. Prepr.* 1972, **13**, 373
28 Chao, H. S. I. *Polym. Bull.* 1987, **18**, 131
29 White, D. M. *Compreh. Polym. Sci.* 1989, **5**, 473
30 White, D. M. *Macromolecules* 1979, **12**, 1008
31 McKillop, A., Fiand, J. C. and Hug, R. P. *Tetrahedron* 1974, **30**, 1373
32 Trent, J. S., Scheinbein, J. I. and Couchman, P. R. *Macromolecules* 1983, **16**, 589
33 Paul, D. R. and Barlow, J. W. *J. Macromol. Sci., Rev. Macromol. Chem.* 1980, **18**, 109
34 ten Brinke, G., Karasz, F. E. and MacKnight, J. W. *Macromolecules* 1983, **16**, 1827
35 Paul, D. R. and Barlow, J. W. *Polymer* 1984, **25**, 487
36 Kammer, H. W. and Kressler, J. *Makromol. Chem., Macromol. Symp.* 1988, **18**, 63
37 Kressler, J., Kammer, H. W., Morgenstern, U., Litauski, B., Berger, W. and Karasz, F. E. *Makromol. Chem.* 1990, **191**, 243
38 Walsh, D. J. and Rostami, S. *Adv. Polym. Sci.* 1985, **70**, 119
39 Rösch, J., de Lucca Freitas, L. L. and Stadler, R. submitted
40 Cheng, S. Z. D. and Wunderlich, B. *Macromolecules* 1987, **20**, 1630
41 Aycock, D., Abolins, V. and White, D. M. in 'Encyclopedia of Polymer Science and Technology', Wiley, Chichester, 1988, Vol. 13
42 Koenhen, D. M., Bakker, A., Broens, L., van den Berg, J. W. A. and Smolders, C. A. *J. Polym. Sci., Polym. Phys. Edn.* 1984, **22**, 2145
43 Wenig, W., Hammel, R., MacKnight, W. J. and Karasz, F. E. *Macromolecules* 1976, **9**, 253
44 Annighöfer, F. and Gronski, W. *Colloid Polym. Sci.* 1983, **261**, 15
45 Stadler, R. and Gronski, W. *Colloid Polym. Sci.* 1983, **261**, 215
46 Caplan, D. S. *J. Appl. Polym. Sci.* 1976, **20**, 2615
47 Ward, I. M. 'Mechanical Properties of Solid Polymers', 2nd Edn., Wiley, Chichester, 1985
48 Auschra, C. *Doctoral Dissertation* Mainz, 1992
49 Shull, K. R., Kramer, E. J., Hadziioannou, G. and Tang, W. *Macromolecules* 1990, **23**, 4780
50 Shull, K. R., Winey, K. I., Thomas, E. L. and Kramer, E. J. *Macromolecules* 1991, **24**, 2748
51 de Araujo, M. A., Stadler, R. and Cantow, H. J. *Polymer* 1988, **29**, 2235
52 Brown, H. R., Char, K. and Deline, V. R. *Macromolecules* 1990, **23**, 3383
53 Auschra, C., Stadler, R. and Voight-Martin, I. G. *Polymer* 1993, **34**, 2094